Thin–Walled Structures 158 (2021) 107157

Contents lists available at ScienceDirect

Thin-Walled Structures

journal homepage: http://www.elsevier.com/locate/tws

Full length article

Behaviour of continuous fibre composite sandwich core under low-velocity impact

Sartip Zangana [a,*], Jayantha Epaarachchi [a], Wahid Ferdous [b], Jinsong Leng [c], Peter Schubel [b]

[a] University of Southern Queensland, Centre for Future Materials (CFM), School of Mechanical and Electrical Engineering, Toowoomba, QLD, 4350, Australia
[b] University of Southern Queensland, Centre for Future Materials (CFM), Toowoomba, QLD, 4350, Australia
[c] Centre of Composite Materials and Structures, Harbin Institute of Technology, Harbin, China

ARTICLE INFO

Keywords:
Novel composite core
Impact behaviour
Impact damage
Finite element modelling
Empirical prediction

ABSTRACT

This article describes an experimental study of the impact behaviour of a novel composite corrugated core sandwich structure under low-velocity impact. Influences of geometric parameters of the novel sandwich core, such as thickness, height, and short span length were studied. Four different configurations of composite corrugated core sandwich structures were prepared and tested. The impact events were monitored using a high-speed camera and measured by an impact force transducer and accelerometer attached to the impactor. The results revealed that the increase of core thickness improved impact capacity while the increase of core height decreased sandwich strength by increasing elastic deformation. The damage status of the novel composite core sandwich was simulated and insight into the damage mechanism was gained with finite element analysis. This study proposes an improved numerical model by incorporating the effect of the impactor head which was able to predict the impact capacity to within 10% variation of the experimental results. The results also identified that the multi-cell composite corrugated core increased the impact capacity due to the continuity of the fibres between adjacent cells. Moreover, the trapezoidal composite corrugated sandwich core showed higher specific strength compared to traditional honeycomb, truss and foam cores.

1. Introduction

Sandwich panels have been used in lightweight structures including transportation vehicles, aircraft wings, floor pans and body panels due to their high specific stiffness-to-weight ratio [1–3]. So far, researchers have investigated the mechanical behaviours of sandwich panels manufactured from metal foam core [4], aluminium corrugated core [5–7] and steel core [8–11]; however, a major problem with these metallic core sandwiches is their heavy weight. The weight penalty can be minimised using lightweight materials such as fibre reinforced composite materials. The fibre composite cores are a new generation structural component, which can be tailored to address any challenging engineering hurdles.

The concept of a hybrid sandwich structure also gained the attention of researchers to save weight, by combining metal with composite materials in sandwich fabrication. For example, aluminium honeycomb cores were combined with carbon fibre laminated skins with rubber [12,13] and their mechanical properties were investigated under low-velocity impact. As well, the failure mode of such a structure was investigated [14]. Furthermore, impact behaviours of a hybrid sandwich comprising an aluminium corrugated core and carbon-fibre composite skin were also investigated [15–17].

A number of researchers have recently investigated composite core sandwich panels, including foam composite sandwich [18–20], composite honeycomb sandwich [21–25], tubular composite structures with/without honeycomb sandwich core [26], composite pyramidal truss core sandwich [27], and composite triangular corrugated core sandwich [28], and Taghizadeh et al. [29] experimentally investigated the mechanical properties of PVC foam-filled corrugated sandwich composite under quasi-static compression load and compared these with foam sandwich. They observed the structural efficiency of the PVC foam-filled corrugated sandwiches is higher than that of the foam sandwich. Zhang et al. [30] investigated the dynamic crushing behaviour of a carbon-fibre composite sandwich with different reinforcing materials, and their study found that the size of the damaged zone is largely affected by the core materials. Torre et al. [31] compared the impact response of traditional composite foam core sandwich with a reinforced foam core, finding that the latter sandwich enhanced core

* Corresponding author.
E-mail addresses: Sartip.Zangana@usq.edu.au (S. Zangana), Wahid.Ferdous@usq.edu.au (W. Ferdous).

https://doi.org/10.1016/j.tws.2020.107157
Received 24 March 2020; Received in revised form 16 September 2020; Accepted 17 September 2020
Available online 8 October 2020

crashworthiness with better performance in terms of impact strength and impact energy absorption capability. Therefore, it can be said that the fibre composite core has great potential to minimise the current challenge by improving mechanical behaviours.

The anisotropic behaviour [32] with high contact area between the core and face sheets [33] are important factors to give attention to the trapezoidal composite corrugated core sandwich among all the composite sandwich cores. Several parameters affect the structural performance of such composite sandwich panels. Zhang et al. [33] found that the increase of core thickness enhanced the specific bending strength of the composite sandwich structure while increasing contact length between the core and upper face sheet led to a decrease in the specific bending strength. Torre et al. [34] compared fluted composite core with foam composite core under drop weight tests and the found the former has better mechanical behaviours. Schneider et al. [35] investigated the high-velocity impact behaviour of low- and high-density non-continuous trapezoidal composite core sandwich. They observed that the core density has a significant influence on the sandwich strength. In another study Schneider et al. [36] employed high-velocity impact to investigated impact behaviour of sandwich beam fabricated from trapezoidal composite core. They found that the impact behaviours of such sandwich can be enhanced by reinforcing interface between the face sheet and core web. Kazemahvazi et al. [37] investigated the high-velocity impact response of non-continuous inclined core struts fabricated from carbon-fibre epoxy. Although they investigated the effect of core thickness-to-length, their study was limited to utilising only two inclined core struts to represent continuous trapezoidal core members, which is not the true representation of real scenarios in the field. Russell et al. [38] carried out high-velocity impact tests on unfilled and foam-filled glass/fibre triangular composite corrugated core structures and observed uniform deformation of the specimens; foam filling had nearly no influence on the impact behaviours of the corrugated cores. Song et al. [39] experimentally and numerically investigated the skin-stringer interface failure of composite panels under high-velocity impact. The results showed that initial delamination always occurred at the skin-stringer interface of the panel, and this delamination was located away from the impact area. In another study, an experimental impact test was conducted to investigate the compressive strength of damaged graphite/epoxy hat stiffened panels after low-velocity impact [40]. The authors suggested that both invisible and extensive visible damage reduced the ultimate strength of the panels.

The literature showed that the research on the trapezoidal composite corrugated core sandwich has been mostly limited to metal trapezoidal core or to non-continuous composite trapezoidal core, under quasi-static loading condition to investigate geometrical parameters, and failure mode. To date, there has been no dependable evidence resulting from the investigation of single-cell and multi-cell continuous trapezoidal composite corrugated sandwich core under low-velocity impact, given that the composite core sandwich is more vulnerable to low-velocity impact during its service life [41]. To fill this knowledge gap, this study investigated the impact behaviour, energy absorption capacity, and failure mode of a trapezoidal composite corrugated core sandwich with different core geometrical parameters.

Moreover, this study aims to provide a conceptual prediction of impact capacity for trapezoidal composite corrugated core sandwich and also performed numerical modelling to better understand the failure mechanism. Subsequently, the work has extended to investigate the performances of the multi-core sandwich structures under low-velocity impact event. The outcome of this study will contribute to the scientific knowledge in the area of impact behaviour of composite core sandwiches and help engineers when designing this type of structure.

2. Materials and design of experiments

2.1. Materials and fabrication

Fig. 1(a) illustrates the schematic diagram of the proposed corrugated core. The specimens were fabricated from woven E-glass fibre [0/90] and epoxy resin (Kinetix R246TX) with the fibre volume fraction of 42%. Three different wooden moulds were utilised (see Fig. 1(b)–(d)) to fabricate four different designs of composite sandwich (D1-D4). The wet hand-layup technique was used to fabricate the upper and lower face sheets and corrugated core. Constant pressure was employed on the corrugated core mould to ensure uniform core angle and thickness. The plies stacking sequence of the face sheets and corrugated core was $[0/90]_{2S}$ for D1 and D4 and $[0/90]_{3S}$ for D3 and D4. Four plies of woven E-glass fibre were used in fabrication of each member of D1 and D4 configuration, while D2 and D3 were fabricated from six plies. The warp and weft fibres were laid in the X and Z directions, respectively, while the height of the composite corrugated core sandwich was aligned in the Y direction. The corrugated core, upper face, and lower face sheet were cured up to 48 h before demoulding. To construct a composite core sandwich panels, the parts were bonded together by using adhesive techniglue (100 g R5 with 26 g H5). The fabricated panels were cut into three equal specimens with average width of 35.45 mm in the Z-direction. Four different categories of corrugated core sandwich structures (D1 to D4 in Fig. 1(e)) with three replicates in each geometry were fabricated. The weight of D1 configuration was less than the D2 and D3 by 30%, this is attributed to less thickness of the sandwich member (upper and lower skins and core) due to fabrication of D1 from four layers of glass fibre, while six layers were used in fabrication of D2 and D3. The design parameters of the composite trapezoidal corrugated core sandwich specimens are summarised in Table 1.

3. Experimental program

Low-velocity impact tests on trapezoidal composite corrugated core sandwich structures were conducted by using a drop-weight impact system (Fig. 2) in accordance with ASTM-D7136 [42]. The designated kinetic energy was above the visible damage threshold of the upper face sheet and core flat member based on Eq. (1) of the standard [42].

$$E = t.CE \tag{1}$$

where, t is the summation of the thicknesses of the upper face sheet and the core whereas CE is the specific ratio of impact energy to specimen thickness (6.7 J/mm). Four different configurations (D1-D4) of trapezoidal woven E-glass fibre epoxy composite corrugated core sandwich were tested. For D1, D2 and D3 specimens, the kinetic energy (KE) of the impactor was set to 40 J. Here the critical impact energy for the composite structures was increased by 30% above the threshold impact energy of the parent material of D2 and D3 specimens [20,42]. The kinetic energy was in the range of low-velocity impact events [41]. Three different heads (flat, hemispherical and conical) with 12 mm diameter for each were used for impacting D1-D3 specimens. The D4 specimen was impacted at 25 J of threshold impact energy of original materials then this was increased by 30% and 60% of the threshold impact energy to 32.5 J and 40 J by using a 12 mm hemispherical impactor head (HH). Table 2 shows the experimental setup of impact tests. The corrugated core was laid on a rigid steel plate and clamped at two sides using jaw clamps while adjustable wood parts were attached between the upper and lower face sheets of the structure, as shown in Fig. 2. A piezoelectric (PCB-200C20) load cell was used to measure the instant impact force and it was placed in between the impactor mass and the impactor head to obtain the actual responses of the core. An accelerometer (PCB-5014B) was attached to the impactor mass to measure the acceleration. The double integration to acceleration-time provided the displacement of the impactor nose. Siemens-LMS SCADAS frame was

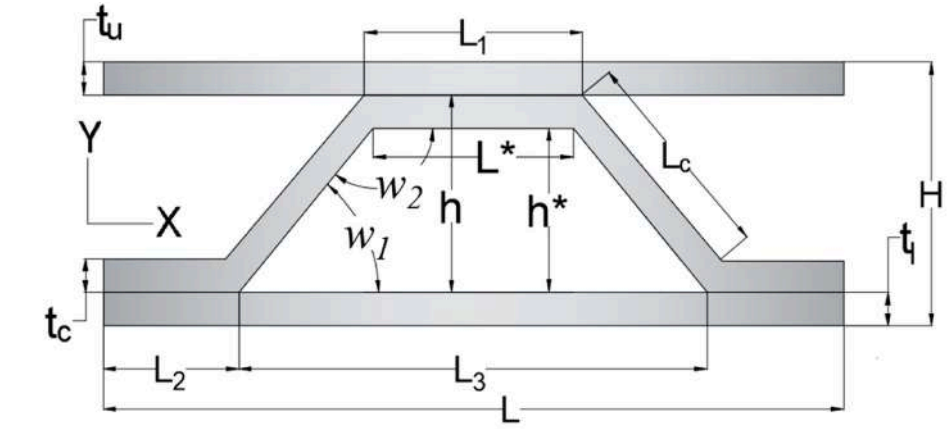

L	Unit cell length	h	Core height
L_1	Short span length	h*	Mold height
L*	Upper mold length	t_u	Upper face sheet thickness
L_2	Lower mold length	t_c	Core thickness
L_3	Long span length	t_l	Lower face sheet thickness
L_c	Core struts length	w_1	Lower core angle
H	Sandwich height	w_2	Upper core angle

(a)

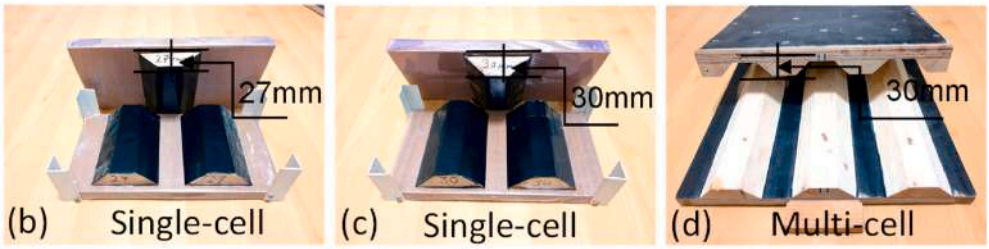

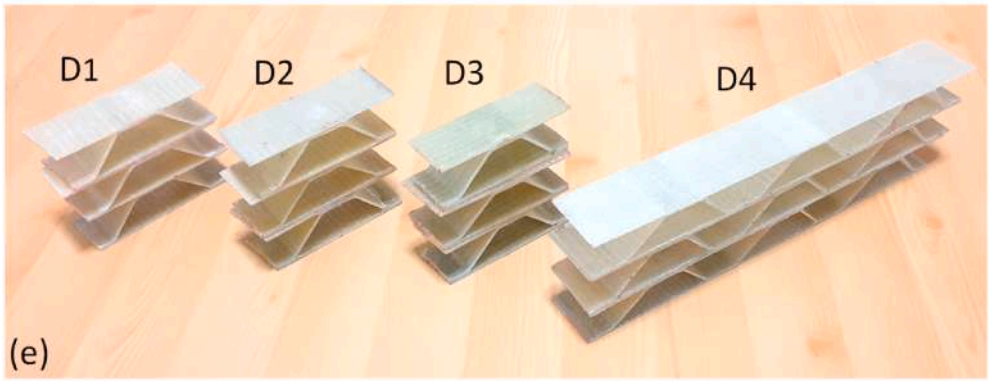

Fig. 1. Composite corrugated core sandwich specimens (a) schematic diagram and geometrical parameters, (b) corrugated core moulds, (c) single-cell sandwich, and (d) multi-cell sandwich.

Table 1
The parametric geometry of the composite corrugated core sandwiches.

Core Design	Qty	t_c (mm)	h (mm)	L_1 (mm)	$t_u = t_l$ (mm)	H (mm)	S.W* (gm)
D1	3	1.75	28.5	32.2	1.9	32	28.1
D2	3	2.1	29.1	33.3	2.4	34	40.6
D3	3	2.1	32.1	27.1	2.4	37	40.3
D4	3	1.75	28.5	32.1	1.9	32	93

The symbol (*) refers to the average value, and S.W is the sandwich weight.

utilised to obtain the force-time and acceleration. As in Ref. [33], the absorbed energy by the sandwich panel was estimated by Eq. (2).

$$AE = \int_0^{\delta} p(t)d\delta \tag{2}$$

where, P and δ are the force and the impactor displacement, respectively. The rebound energy of all cases was not considered in this study. A high-speed camera, of frame rate 1000 frames per second, (Sony-RX100Y) was used to observe the impact event and entire deformation response of the specimen.

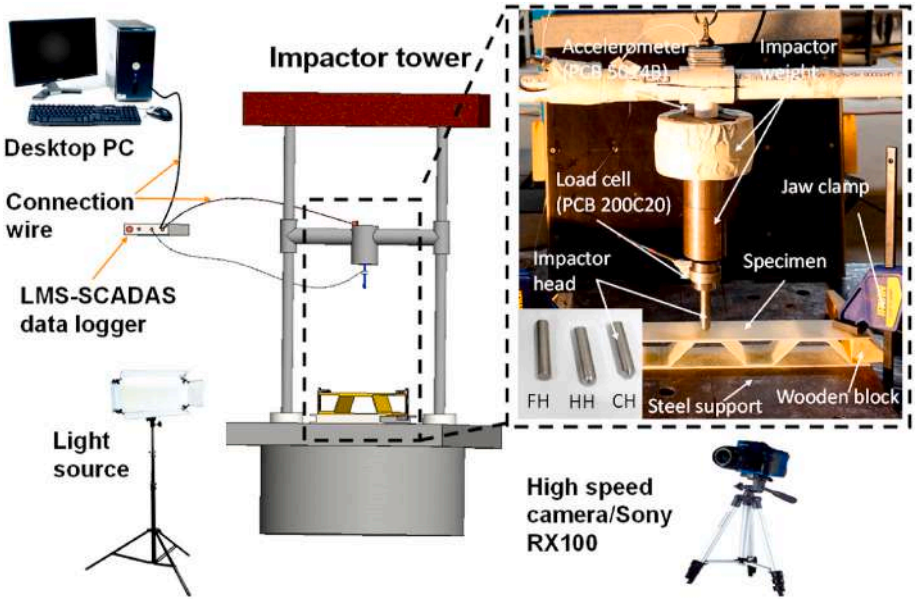

Fig. 2. Experimental setup of low-velocity impact test of the trapezoidal composite corrugated core structure.

Table 2
Experimental setup of low-velocity impact tests.

Core Design	Qty	Impactor			K.E (J)	Above threshold K.E (%)
		Head	Mass (kg)	Velocity (m/s)		
D1	3	FH, HH, CH	4	4.47	40	60%
D2	3	FH, HH, CH	4	4.47	40	30%
D3	3	FH, HH, CH	4	4.47	40	30%
D4	1	HH	2.5	4.47	25	0%
D4	1	HH	3.25	4.47	32.5	30%
D4	1	HH	4	4.47	40	60%

** FH, HH, and CH are flat, hemispherical and conical impactor heads, respectively.

4. Results and discussion

4.1. Effect of core thickness

The effect of the core thickness (t_c) has been investigated from the results of D1 and D2 specimens. Fig. 3(a)–(c) show the impact force vs time response of the D1 and D2 designs of the composite corrugated sandwiches. All the cases showed an abrupt drop of force after the initial peak load. This is attributed to the local damage caused by the impact and subsequent elastic buckling of the core struts. Then the impact force increased again to second peak load followed by another force drop due to core struts crashing. This phenomenon was predominant in the impact with FH and HH. It was observed that the impact load increased again (Fig. 3(a) and (b)) due to the flexural resistance of the upper face sheet in most of the cases. This phenomenon indicates the core crush, which mitigates the impact energy flow by delayed face sheet bending. This can be attributed to the same mechanical properties and the thickness of the upper face sheet and core struts.

Fig. 3(a)–(c) also revealed that the sandwich systems of D1 and D2 exhibited different magnitudes of the peak impact force with an approximately similar trend of loading response. Increasing the core thickness from 1.75 to 2.1 mm led to an increased peak force value of between 35 and 45% with all impactor head types. However, the impact time response of D1 was longer than D2 due to the rapid core crush of D1. It can be seen that the impact force has a noticeable fluctuation when the impactor was in contact with the core. This phenomenon can be attributed to the matrix cracking, fibre breakage, and delamination of the core structure [43–45]. The same configuration of composite core sandwich (for example D1) showed highest impact resistance with FH, followed by HH and CH. This is attributed to the decreasing contact stiffness parameter which depends on impactor radius [46].

The captured photos also showed a severe fracture of the upper angle of the corrugated core due to combined tensile and shear forces, followed by large deformation of the upper face sheet (Fig. 3(d)–(h)). However, the thicker core struts of D2 did not show core buckling and crushing due to the semi-penetration of the conical impactor head while the flexural deformation of the upper face sheet was not observed as shown in Fig. 3(i). This implies the buckling of the core affected by the core thickness and depending on the magnitude of the thickness it may or may not occur before impact damage. The closer look at Fig. 3(g) and (i) can reveal that the dust cloud on the top skin and the core members due to the impact event have shown a perfect impact force distribution. Therefore, it can be concluded that the increase of core thickness can increase sandwich impact resistance and reduce impact time, core buckling, and core crushing at the upper angle, as shown in Fig. 3(d) and (i).

4.2. Effect of core height and short span length

The influences of the core height (h) and short span length (L_1) on the corrugated core sandwich response (in D2 and D3) under low-velocity impact were investigated under an impact force at constant kinetic energy of 40 J. Fig. 4(a)–(c) indicate that the core height has a significant effect on the impact behaviour of the composite core. A close inspection of the curve response revealed that the impact peak force decreased with increasing core height. Fig. 4(a)–(c) also show that the impact time response of D3 was longer than that of D2 due to the considerable movement of the impactor nose accompanied by large deformation of the upper face sheet. The slipping of the upper face sheet of the sandwich under jaw clamp might cause also a slight difference between the impact times. The captured photos in Fig. 4 indicate that the upper angle of the core is the weakest point in the composite trapezoidal corrugated sandwich and this point is where severe damage occurred. This is due to the combination of the exceeded normal shear force in the upper flat part of the core (L_1) and a high bending moment of core struts in upper

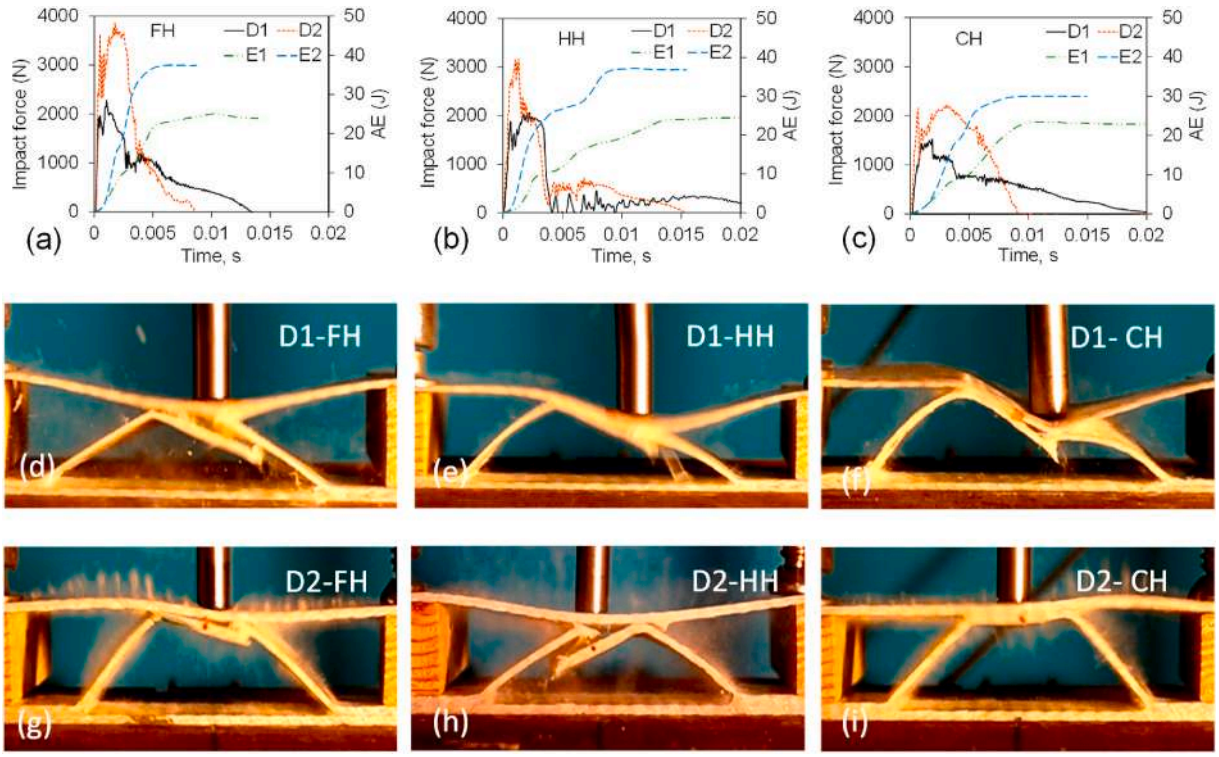

Fig. 3. Impact response at maximum displacement of the impactor head (a–c) impact vs time under the flat, hemispherical and conical heads, (d–f) structural deformation of D1 specimens, and (g–i) structural deformation of D2 specimens.

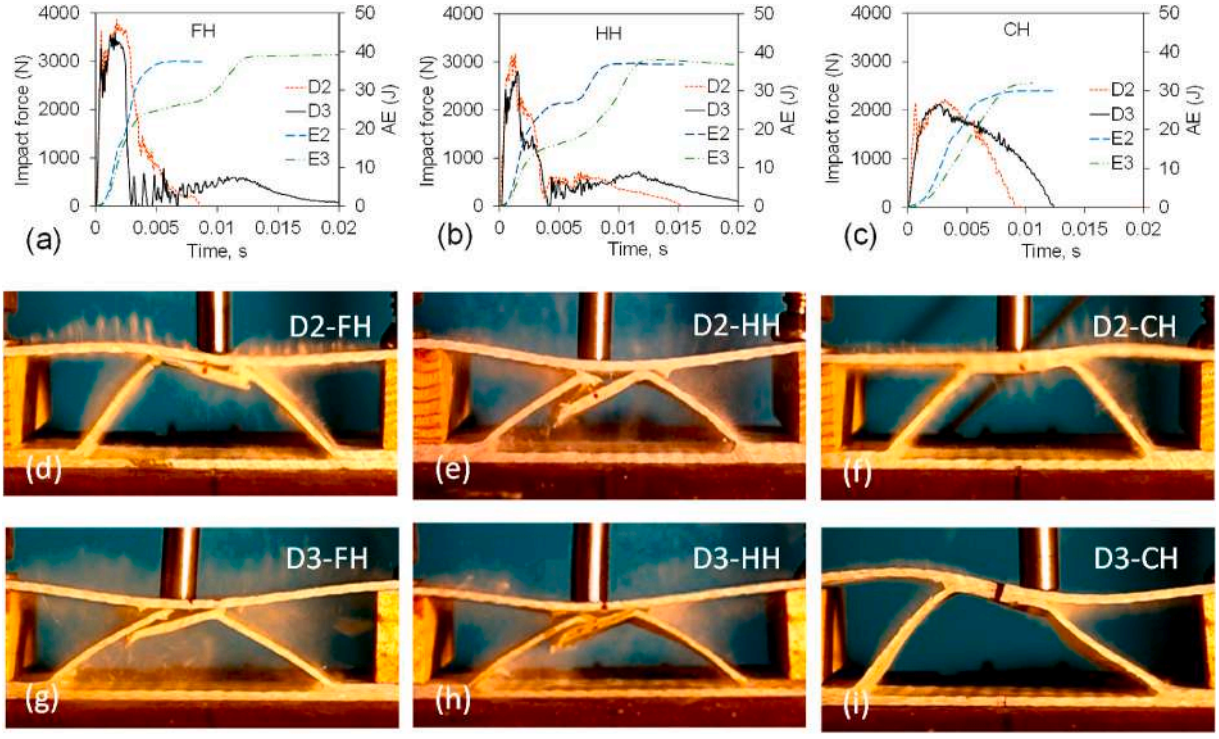

Fig. 4. Impact response at maximum displacement of the impactor head (a–c) impact vs time under the flat, hemispherical and conical heads, (d–f) structural deformation of D2 specimens, and (g–i) structural deformation of D3 specimens.

nodes (w_2) that leads to flattening the core angle; thus, the tensile stress exceeded the tensile strength of the parent material. Increasing the core height significantly increased the impact time and elastic deformation of the sandwich (Fig. 4) by absorbing more kinetic energy exerted at the impact. It can be seen that decreasing the span length (L_1) from 33.3 mm (D2) to 27.1 mm (D3) affected the sandwich impact behaviour by post bending of the upper face sheet (Fig. 4(d)–(i)). The post bending generally causes de-bonding failure at the apex of the traditional

triangular unit corrugated cores [28]. Therefore, a careful selection of span length is an important aspect for the design of corrugated core sandwich.

The energy absorption of the composite corrugated core sandwiches D1, D2, and D3 were calculated by Eq. (2). Fig. 5(a) shows that the increase of core thickness of D1 by 33% as in D2 leads to increasing the energy absorption capacity by roughly 50%, due to the increasing of compression resistance of the core struts. While increasing the core height of D2 by 12% as in D3 increased absorbed energy by 40%, this is attributed to increased core struts buckling.

The most relevant mechanical behaviour of the sandwich structures to consider is the specific energy absorption which is the energy absorbed per unit mass of the materials. This is in order to enhance the energy absorption capability and to design more efficient mechanisms of failure [33]. The specific energy absorption values (SEA), which were calculated from the absorbed energy normalised by the total sandwich weight [30], are shown in Fig. 5(b). It can be seen that the increase of core height significantly affected the energy absorption capability of the corrugated core composite sandwich. However, the sandwich weight had no noticeable effect on the SEA of the composite core sandwich, which ranged between 0.85 and 0.95. This is attributed to the increase of the upper and lower face sheets' weight with increasing core weight.

4.3. Impact damage evaluation using finite element modelling

A three-dimensional (3-D) finite element model was created for D2 specimens by explicit dynamics ANSYS-R19.1 Workbench ACP-pre/post to investigate the effect of impactor head on damaged trace of the trapezoidal composite corrugated core sandwich under low-velocity impact. The damaged traces of D2 configuration due to different impactor heads were compared with finite element modelling, to obtain a clear and visible view of their damage trace.

The mechanical properties of glass fibre reinforced epoxy composite material were taken from Ref. [47] and summarised in Table 3. Woven glass fibre $[0/90]_{3s}$ was employed in laminate stacking sequence. The mechanical properties of epoxy were employed to simulate the contact between the layers, this can be chosen from the ACP-pre facility. Four different modes of failure (compressive fibre failure, tensile fibre failure, compressive matrix failure and tensile matrix failure) were evaluated using Hashin failure criteria [48]. The expected failures of the specimens are within the scope of Hashin failure criteria. Moreover, previous researchers used Hashin failure criteria to evaluate failure mechanism in woven composite materials [15,49], which is why the authors used Hashin failure criteria. Instant stiffness reduction was used [50] to consider damage evolution, and once the principle stress reached the ultimate value the composite materials, stiffness degraded by 0.8 [51]. The eight-node Solid-Shell element (SOLSH190) and eight-node Solid element (SOLID185) were chosen for meshing the sandwich structure and impactor head, respectively. The total number of elements of the structure and the impactor head were 136600 and 8500, respectively while the element size was approximately 1 mm with an aspect ratio close to one. A frictionless contact of a rigid impactor head with the composite sandwich was created from structural steel material. The experimental specimens were not entirely fixed at both edges even with the provision of clamp supports. However, the very accurate determination of degree of freedom for such support is a challenge. Therefore, the rotation and translation at the support and composite sandwich edges were constrained to simulate the experimental setup as close as possible with large geometrical deformation was permitted. The impactor mass and velocity were 4 kg and 4.47 m/s, respectively, to ensure 40 J of impact energy.

Table 3
Mechanical properties of composite laminate fabricated from E-glass/fibre reinforced epoxy - average value [30].

Symbol	Property	Value	Unit
$E_{11,}$	Young's modulus in the longitudinal direction	48.14	GPa
E_{22}	Young's modulus in the transverse direction	48.14	GPa
E_{33}	Young's modulus in the thickness direction	12.2	GPa
$\nu_{12,}$	In-plane Poisson's ration	0.05	
ν_{23},ν_{13}	Through thickness Poisson's ration	0.2	
G_{12}	In-plane shear modulus	5.8	GPa
$G_{23,}$ G_{13}	Through thickness shear modulus	2.1	GPa
X_T	Tensile strength in longitudinal direction	1022	MPa
X^C	Compressive strength in longitudinal direction	490	MPa
Y^T	Tensile strength in transverse direction	1022	MPa
Y^C	Compressive strength in transverse direction	490	MPa
S^L	Shear strength in longitudinal direction	22.8	MPa
S^T	Shear strength in transverse direction	22.8	MPa

The impactor movement was enabled in the Z-direction and restricted in both X- and Y-directions. The failure status value ranged between 0, 1 and 2, which means no damage, partially damage and fully damaged, respectively. On the other hand, the matrix compressive failure criterion value ranged between 0 and 1, with 0 meaning no failure, and 1 indicating a fully damaged matrix [52]. The tensile and compressive properties were assumed to be the same in both longitudinal and transverse directions due to 0/90 woven fibre orientations.

Fig. 6 shows the numerical damage status of the trapezoidal composite corrugated core sandwich under low-velocity impact. The full damage status of the flat head has a circular shape with protrusion towards core struts. This is attributed to core struts reaction, which caused a transfer of part of the impact energy to local damage on the impacted surface. Furthermore, it can be seen that the flat head produced larger damage while the hemispherical impactor created smaller damage on the impacted surface and the conical head produced the least damage, this is due to the semi-penetration of the impacted composite surface. Moreover, the semi-penetration damage reduced the partial damage status on the upper face sheet. It can be concluded that the variety of impactor head shapes, even with a constant impact energy level, can produce different impact traces on the trapezoidal composite corrugated core sandwich.

Fig. 7(a)–(c) show impact traces of the upper face sheet under low-velocity impact with three impactor heads. A whiteness ring of

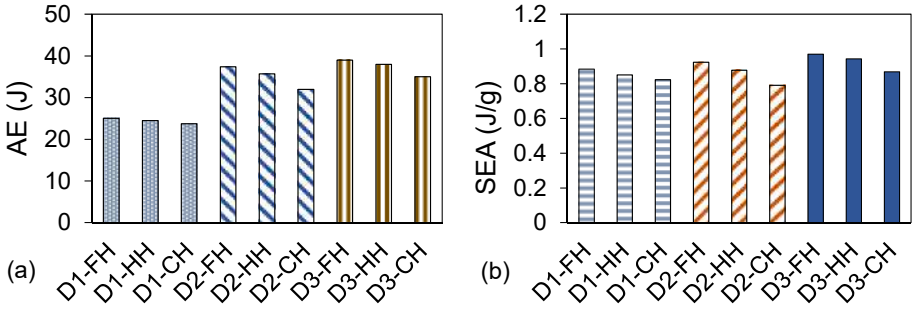

Fig. 5. (a) Absorbed energy of D1, D2, and D3 sandwich core configurations (b) Specific energy absorption of D1, D2, and D3 sandwich core configurations.

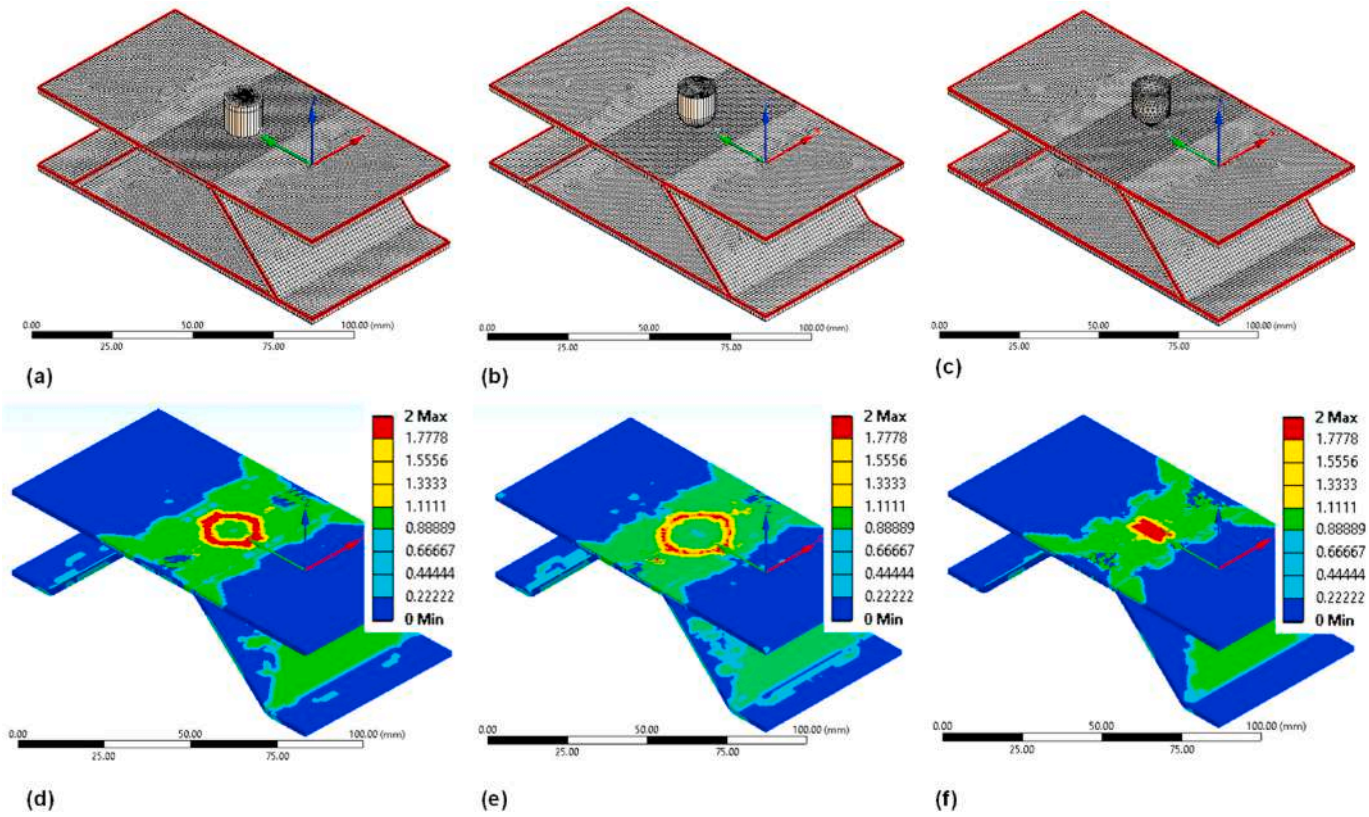

Fig. 6. Finite element modelling of trapezoidal composite corrugated core sandwich under low-velocity impact: (a–c) composite sandwich model with flat, hemispherical, and conical impactor heads, respectively; (d–f) impact damage status of the composite sandwich with flat, hemispherical, and conical impactor heads, respectively.

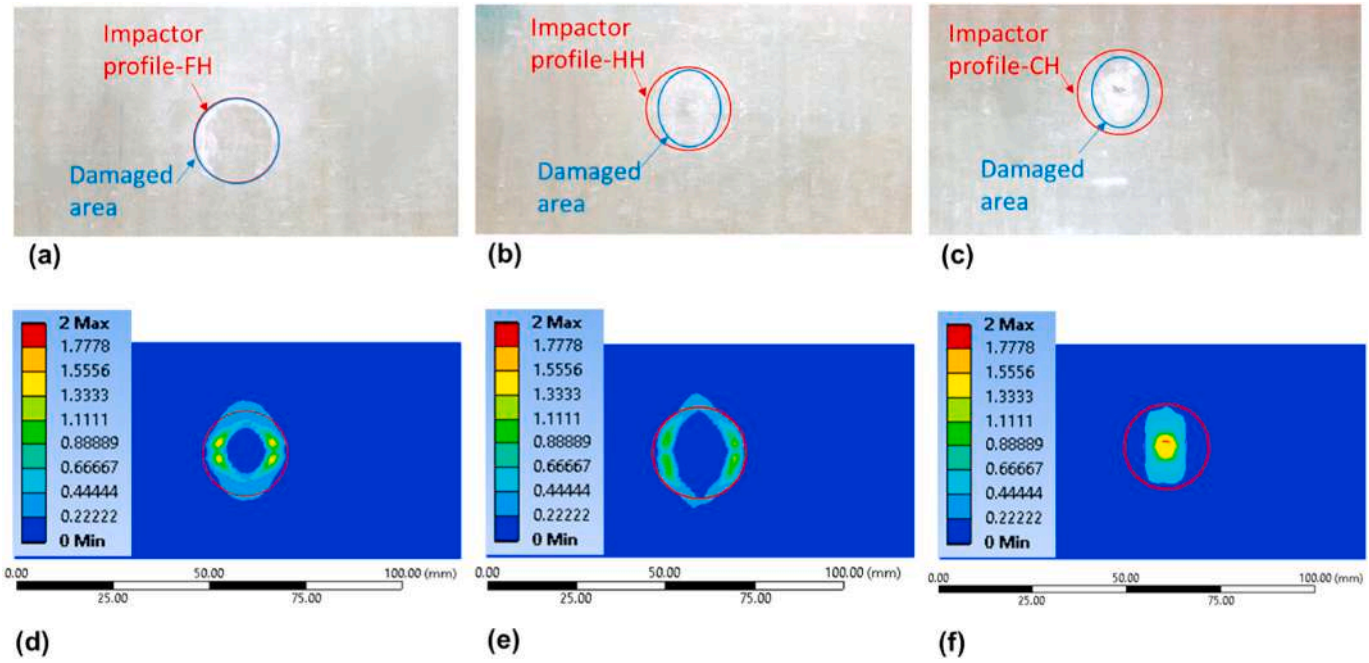

Fig. 7. Damage trace of tested specimens and numerical results of the upper face sheet of the trapezoidal composite corrugated core sandwich under low-velocity impact: (a–c) experimental photos with flat, hemispherical, and conical impactor heads, respectively; (d–f) numerical images with flat, hemispherical, and conical impactor heads, respectively.

damage, which refers to matrix damage [53], is identical to the impactor head profile. The damage traces of the hemispherical and conical heads were less than the area of impactor profile by approximately 10% and 30%, respectively. Fig. 7(d)–(f) show numerical model correlation with experimental damage of the sandwich upper face sheet. Due to the whiteness of the impact area, which refers to microscopic matrix

damage [54], the matrix compressive failure criterion of the impacted area was investigated and compared with the experimental results. As shown in Fig. 7(d)–(f), the flat head produced large full matrix compressive failure, while both hemispherical and conical heads created full matrix compressive failure, but less than the impactor profile. It can be seen that the 3-D finite element models showed good agreement with the experimental results in terms of damage trace on the upper face of the trapezoidal composite corrugated core sandwich using different impactor heads under low-velocity impact.

4.4. Predicting impact capacity

The initial peak forces in the linear part of the experimental results were predicted by modifying the equation given by Malcom et al. [55]. When the specimens were impacted by a drop weight, the core struts were subjected to axial compression force before failure. The axial compression forces (F) are obtained from the compressive stress equation (Euler formula) of the core struts, as provided in Eqs. (3) and (4). However, the effect of different impactor shape was not considered in the existing model [55]. This study modified the existing equation by introducing the impactor head shape factor in Eq. (3) to make it suitable for different types of impactor heads.

In Eqs. (3) and (4), σ_c and E_c are the core strut stress and Young modulus of the parent materials of the core struts in the fibre direction, respectively, k is the ratio between the effective length and actual core struts length, varying between 0.5 and 1 depending on the end condition of core struts. In this study, k is considered 0.7 due to the assumption of the lower end of the core struts as a fixed point (with no movement of that end due to the rigid plate support) and the upper end of the core struts as a pin end (due to rotation of that point). The S_f is the shape factor which depends on the geometry of the impactor head. On the other hand, t, h, and w_1 are the thickness, height, and angle of the core member, respectively, n is the number of the core strut, and A_c is the cross-section of the core strut.

$$\sigma_c = \frac{\pi^2 E_c}{12k^2.S_f}\left(\frac{t.\sin w_1}{h}\right)^2 \tag{3}$$

$$F = n.A_c.\sigma_c \tag{4}$$

Table 4 compares the theoretical and experimental impact forces (for D2) with and without shape factor. It can be seen that if the shape factor is not considered, the theoretical equation estimated impact forces within 2% accuracy for flat head, 15% for hemispherical head and 51% for conical head. This implies the theoretical equation can reliably predict the impact forces only for flat impactor head. This is because full contact between the impactor head and impacted area was achieved due to the flatness of the head. On the other hand, full contact cannot be achieved for the hemispherical and conical impactor heads. Therefore, the impactor head shape factor was introduced in Eq. (3). Analysing the effective projected contact surface area in Fig. 7, it was found that the shape factor for hemispherical and conical heads is 0.9 and 0.7, respectively, compared to 1 for flat head. The incorporation of impactor head shape factor predicted impact capacity within 10% accuracy for all types of impactor heads investigated in this study.

Table 4
Comparison between experimental initial peak force and theoretical results.

Sample ID	Exp. (N)	Theoretical (N)		Variation (%)	
		Without shape factor	With shape factor	Without shape factor	With shape factor
D1-FH	2260	2195	2195	2	2
D1-HH	2040	2175	1981	−7	2
D1-CH	1674	2154	1556	−28	7
D2-FH	3302	3387	3387	−2	−2
D2-HH	2937	3367	3057	−15	−4
D2-CH	2247	3246	2345	−51	−9
D3-FH	2841	2747	2747	3	3
D3-HH	2266	2632	2376	−16	−4
D3-CH	2052	2612	1902	−27	7

4.5. Comparison of multi-cell and single-cell corrugated core performances

A multi-core sandwich structure (D4) was investigated with different levels of impact forces at energy levels of 25 J, 32.5 J and 40 J to understand the performances of single-core and multi-core structures. Fig. 8(a)–(c) show the impact force time and structural energy absorption of the multi-core composite corrugated sandwich (D4). The force-time response of the multi-core sandwich structure is shown at single and double plateau regions. The behaviour of the first plateau region is attributed to elastic core buckling, and partial de-bonding occurred between the upper face and flat core members (L_1) as shown in Fig. 8(e). The second plateau region shows a flexural bending of the top face plate (Fig. 8(f)). Almost of the impact energy was absorbed, as shown in Fig. 8 (a) and (b). While with kinetic energy of 40J no rebound occurred, however the energy of the sandwich structure reached the capacity of 30 J, and then the core was damaged, which prevented the sandwich from absorbing more than 30 J (Fig. 8(c)). When compared to the single-cell sandwich, the multi-cell sandwich provided good structural integrity and distributing impact forces among adjacent cells. Moreover, the multi-core specimen showed a non-linear but ductile structural behaviour, which has not been seen in the traditional core sandwich structures [53,56].

4.6. A comparison of proposed corrugated composite core with other core structures

The higher the SEA value, the higher the absorbed energy to weight ratio. Table 5 shows the SEA performance of various cores of sandwich structures. The previous study may employed different methods, support conditions or core sizes, however, to overcome this issue the specific energy absorption (SEA) among different sandwich cores were compared. SEA is a normalised form of property regardless of the impactor mass, sample sizes, type and materials of the core.

It can be seen that the proposed composite corrugated core has SEA of 0.88 J/g at 2400 N, which is higher than the other composite cores i.e. the foam core (0.2 J/g at 2500 N) and plastic hollow ball core (0.6 J/g at 2700 N). The proposed trapezoidal composite corrugated core showed a higher SEA value compared to other cores, which means that the proposed corrugated core is better than other core structures. This is due to the elastic buckling of the composite corrugated core struts that allows higher deformation of the sandwich structures and helps absorb more impact energy.

5. Conclusions

Low-velocity impact tests were conducted on four different designs of the trapezoidal composite corrugated core sandwich structures fabricated with E-glass fibres. The influence of geometrical parameters of core struts and multi-cell responses have been investigated. A finite element simulation has been conducted and a modified theoretical model capturing the impact behaviour under different impactor heads has been proposed. The findings of this study can be summarised as below:

- The increase of core thickness increased sandwich impact resistance by reducing core struts buckling. The increase of core height and short span length minimised impact resistance by increasing the elastic deformation of the sandwich.
- The main failure of the continuous trapezoidal composite corrugated core sandwich occurred at the junction of the short span and core

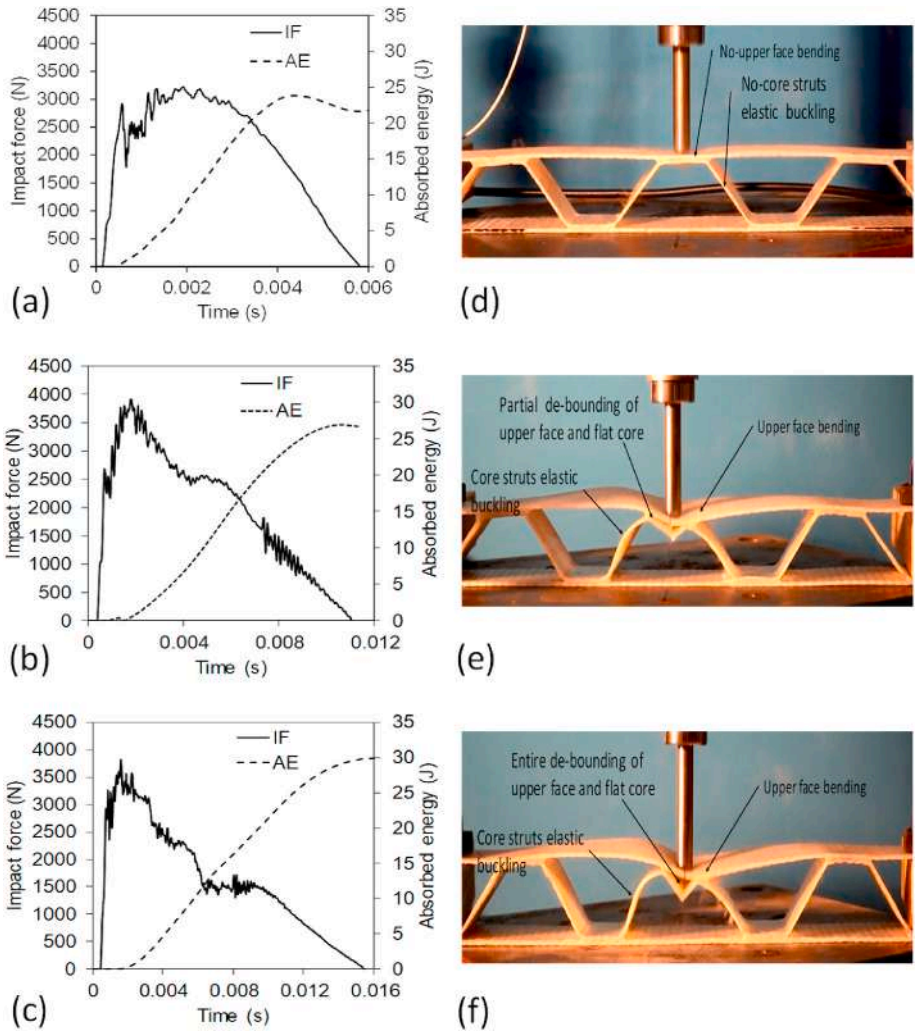

Fig. 8. Low-velocity impact test of D4 sandwich with three different kinetic energy, 25 J, 32.5 J, and 40 J, (a–c) force-time response and (d–f) montage of photographs at maximum displacement.

Table 5
Comparison of single-cell of the composite corrugated core of the current work with published core sandwiches.

Sandwich skins	Core type	I.F(N)	SEA (J/g)
Glass-fibre composite	Composite trapezoidal core (present study)	2400*	0.88*
Carbon-fibre composite	Foam core [57]	2500	0.2**
Carbon-fibre composite	Plastic ball core [30]	2700	0.6
Carbon-fibre composite	Rubber foam ball core [30]	5800	0.2
Carbon-fibre composite	Composite honeycomb core [57]	4000	0.15**
Aluminium	Aluminium honeycomb core [58]	2100	0.1**
Aluminium	Aluminium foam core [58]	2600	0.05**
Steel	Steel sinusoidal core$_{AACC}$ [8]	4200	0.04**

(*) Average value and (**) Calculated.

strut (i.e., at the location of w_2 angle) followed by the flattening of the lower angle (w_1) of the core under low-velocity impact.

- An impactor head shape factor is introduced for reliable prediction. The proposed impactor head shape factors are 1, 0.9 and 0.7 for flat, hemispherical and conical impactor heads, respectively, obtained from experimental observation and confirmed by finite element simulation. The modified empirical model predicted impact forces within 10% deviation of the experimental results, for all types of impactor heads.
- Compared with the single-cell sandwich, the multi-cell sandwich showed higher impact resistance by distributing impact forces among the adjacent cells due to their better structural integrity and composite action.
- The proposed composite core exhibited superior specific energy absorption compared to traditional sandwich cores such as honeycomb, truss, foam, triangular and sinusoidal. The superior performance of the proposed fibre composite core is due to the area of contact between the core and face sheet as well as better fibre continuity at the junction.

Author statement

Sartip Zangana: Data curation, Formal analysis, Investigation, Writing - original draft, Jayantha Epaarachchi: Conceptualization, Methodology, Supervision, Wahid Ferdous: Methodology, Writing - review & editing, Jinsong Leng: Writing - review & editing, Peter Schubel: Writing - review & editing.

Declaration of competing interest

The authors declare that they have no known competing financial

interests or personal relationships that could have appeared to influence the work reported in this paper.

Acknowledgments

The first author would like to acknowledge the financial support from the Ministry of Higher Education and Scientific Research, Iraq. Acknowledgments are also extended to the technical staff at the Centre for Future Materials, University of Southern Queensland, Australia.

References

[1] S. Zangana, J. Epaarachchi, W. Ferdous, J. Leng, A novel hybridised composite sandwich core with Glass, Kevlar and Zylon fibres – investigation under low-velocity impact, Int. J. Impact Eng. 137 (2020) 103430.
[2] A. McCracken, P. Sadeghian, Partial-composite behavior of sandwich beams composed of fiberglass facesheets and woven fabric core, Thin-Walled Struct. 131 (2018) 805–815.
[3] P.R. Oliveira, A.M.S. Bonaccorsi, T.H. Panzera, A.L. Christoforo, F. Scarpa, Sustainable sandwich composite structures made from aluminium sheets and disposed bottle caps, Thin-Walled Struct. 120 (2017) 38–45.
[4] C. Liu, Y.X. Zhang, L. Ye, High velocity impact responses of sandwich panels with metal fibre laminate skins and aluminium foam core, Int. J. Impact Eng. 100 (2017) 139–153.
[5] T. Boonkong, Y.O. Shen, Z.W. Guan, W.J. Cantwell, The low velocity impact response of curvilinear-core sandwich structures, Int. J. Impact Eng. 93 (Supplement C) (2016) 28–38.
[6] C. Kılıçaslan, M. Güden, İ.K. Odacı, A. Taşdemirci, Experimental and numerical studies on the quasi-static and dynamic crushing responses of multi-layer trapezoidal aluminum corrugated sandwiches, Thin-Walled Struct. 78 (2014) 70–78.
[7] C. Kılıçaslan, M. Güden, İ.K. Odacı, A. Taşdemirci, The impact responses and the finite element modeling of layered trapezoidal corrugated aluminum core and aluminum sheet interlayer sandwich structures, Mater. Des. 46 (2013) 121–133.
[8] L. Zhang, R. Hebert, J.T. Wright, A. Shukla, J.-H. Kim, Dynamic response of corrugated sandwich steel plates with graded cores, Int. J. Impact Eng. 65 (2014) 185–194.
[9] L. Zhang, J. Kim, Core crushing and dynamic response of sandwich steel beams with sinusoidal and trapezoidal corrugated cores: a parametric study, J. Sandw. Struct. Mater. 0(0) 1099636217731255.
[10] K. Dharmasena, D. Queheillalt, H. Wadley, Y. Chen, P. Dudt, D. Knight, Z. Wei, A. Evans, Dynamic response of a multilayer prismatic structure to impulsive loads incident from water, Int. J. Impact Eng. 36 (4) (2009) 632–643.
[11] P. Zhang, J. Liu, Y. Cheng, H. Hou, C. Wang, Y. Li, Dynamic response of metallic trapezoidal corrugated-core sandwich panels subjected to air blast loading – an experimental study, Mater. Des. 65 (2015) 221–230.
[12] S.H. Abo Sabah, A.B.H. Kueh, M.Y. Al-Fasih, Bio-inspired vs. conventional sandwich beams: a low-velocity repeated impact behavior exploration, Construct. Build. Mater. 169 (2018) 193–204.
[13] S.H. Abo Sabah, A.B.H. Kueh, M.Y. Al-Fasih, Comparative low-velocity impact behavior of bio-inspired and conventional sandwich composite beams, Compos. Sci. Technol. 149 (2017) 64–74.
[14] S.H. Abo Sabah, A.B.H. Kueh, N.M. Bunnori, Failure mode maps of bio-inspired sandwich beams under repeated low-velocity impact, Compos. Sci. Technol. 182 (2019).
[15] J. Liu, W. He, D. Xie, B. Tao, The effect of impactor shape on the low-velocity impact behavior of hybrid corrugated core sandwich structures, Compos. B Eng. 111 (2017) 315–331.
[16] W. He, J. Liu, S. Wang, D. Xie, Low-velocity impact response and post-impact flexural behaviour of composite sandwich structures with corrugated cores, Compos. Struct. 189 (2018) 37–53.
[17] Y. Rong, W. Luo, J. Liu, Z. Shen, W. He, Effect of core materials on the low-velocity impact behaviour of trapezoidal corrugated sandwich panels, Int. J. Crashworthiness (2019) 1–12.
[18] M. Rezaeifard, S.J. Salami, M.B. Dehkordi, M. Sadighi, A new nonlinear model for studying a sandwich panel with thin composite faces and elastic–plastic core, Thin-Walled Struct. 107 (2016) 119–137.
[19] D. Feng, F. Aymerich, Effect of core density on the low-velocity impact response of foam-based sandwich composites, Compos. Struct. 239 (2020).
[20] R. Mohmmed, F. Zhang, B. Sun, B. Gu, Finite element analyses of low-velocity impact damage of foam sandwiched composites with different ply angles face sheets, Mater. Des. 47 (2013) 189–199.
[21] X. Zhang, F. Xu, Y. Zang, W. Feng, Experimental and numerical investigation on damage behavior of honeycomb sandwich panel subjected to low-velocity impact, Compos. Struct. 236 (2020).
[22] A. Riccio, A. Raimondo, S. Saputo, A. Sellitto, M. Battaglia, G. Petrone, A numerical study on the impact behaviour of natural fibres made honeycomb cores, Compos. Struct. 202 (2018) 909–916.
[23] A. Paul Praveen, V. Rajamohan, A.B. Arumugam, S.S. Rahatekar, Assessment of dynamic properties of hybrid ribbon reinforced multifunctional composite sandwich plates: numerical and experimental investigation, Thin-Walled Struct. 145 (2019).
[24] K. Fu, H. Wang, L. Chang, M. Foley, K. Friedrich, L. Ye, Low-velocity impact behaviour of a shear thickening fluid (STF) and STF-filled sandwich composite panels, Compos. Sci. Technol. 165 (2018) 74–83.
[25] C.C. Foo, L.K. Seah, G.B. Chai, A modified energy-balance model to predict low-velocity impact response for sandwich composites, Compos. Struct. 93 (5) (2011) 1385–1393.
[26] C. Zhang, K.T. Tan, Low-velocity impact response and compression after impact behavior of tubular composite sandwich structures, Compos. B Eng. 193 (2020).
[27] K. Djama, L. Michel, A. Gabor, E. Ferrier, Mechanical behaviour of a sandwich panel composed of hybrid skins and novel glass fibre reinforced polymer truss core, Compos. Struct. 215 (2019) 35–48.
[28] M.R.M. Rejab, W.J. Cantwell, The mechanical behaviour of corrugated-core sandwich panels, Compos. B Eng. 47 (2013) 267–277.
[29] S.A. Taghizadeh, A. Farrokhabadi, G. Liaghat, E. Pedram, H. Malekinejad, S. F. Mohammadi, H. Ahmadi, Characterization of compressive behavior of PVC foam infilled composite sandwich panels with different corrugated core shapes, Thin-Walled Struct. 135 (2019) 160–172.
[30] Y. Zhang, Z. Zong, Q. Liu, J. Ma, Y. Wu, Q. Li, Static and dynamic crushing responses of CFRP sandwich panels filled with different reinforced materials, Mater. Des. 117 (2017) 396–408.
[31] L. Torre, J.M. Kenny, Impact testing and simulation of composite sandwich structures for civil transportation, Compos. Struct. 50 (3) (2000) 257–267.
[32] C. Thill, J. Etches, I. Bond, K. Potter, P. Weaver, Composite corrugated structures for morphing wing skin applications, Smart Mater. Struct. 19 (12) (2010) 124009.
[33] J. Zhang, P. Supernak, S. Mueller-Alander, C.H. Wang, Improving the bending strength and energy absorption of corrugated sandwich composite structure, Mater. Des. 52 (2013) 767–773.
[34] L. Torre, J. Kenny, Impact testing and simulation of composite sandwich structures for civil transportation, Compos. Struct. 50 (3) (2000) 257–267.
[35] C. Schneider, S. Kazemahvazi, D. Zenkert, V.S. Deshpande, Dynamic compression response of self-reinforced poly(ethylene terephthalate) composites and corrugated sandwich cores, Compos. Appl. Sci. Manuf. 77 (2015) 96–105.
[36] C. Schneider, S. Kazemahvazi, B.P. Russell, D. Zenkert, V.S. Deshpande, Impact response of ductile self-reinforced composite corrugated sandwich beams, Compos. B Eng. 99 (2016) 121–131.
[37] S. Kazemahvazi, B.P. Russell, D. Zenkert, Impact of carbon fibre/epoxy corrugated cores, Compos. Struct. 94 (11) (2012) 3300–3308.
[38] B.P. Russell, A. Malcom, H.N. Wadley, V. Deshpande, Dynamic compressive response of composite corrugated cores, J. Mech. Mater. Struct. 5 (3) (2010) 477–493.
[39] Z. Song, J. Le, D. Whisler, H. Kim, Skin-stringer interface failure investigation of stringer-stiffened curved composite panels under hail ice impact, Int. J. Impact Eng. 122 (2018) 439–450.
[40] M.D. Rhodes, J.G. Williams, J.H. Starnes Jr., Effect of Low-Velocity Impact Damage on the Compressive Strength of Graphite-Epoxy Hat-Stiffened Panels, National aeronautics and space administration hampton va langley research, 1977.
[41] G. Davies, R. Olsson, Impact on composite structures, Aeronaut. J. 108 (1089) (2004) 541–563.
[42] ASTM-D7136, Standard Test Method for Measuring the Damage Resistance of a Fiber-Reinforced Polymer Matrix Composite to Drop-Weight Impact Event, ASTM International, USA, 2012.
[43] Z. Li, A. Khennane, P.J. Hazell, A.D. Brown, Impact behaviour of pultruded GFRP composites under low-velocity impact loading, Compos. Struct. 168 (2017) 360–371.
[44] Z.a. Zhang, M. Richardson, Low velocity impact induced damage evaluation and its effect on the residual flexural properties of pultruded GRP composites, Compos. Struct. 81 (2) (2007) 195–201.
[45] S.-X. Wang, L.-Z. Wu, L. Ma, Low-velocity impact and residual tensile strength analysis to carbon fiber composite laminates, Mater. Des. 31 (1) (2010) 118–125.
[46] S. Abrate, Modeling of impacts on composite structures, Compos. Struct. 51 (2) (2001) 129–138.
[47] L.L. Clements, R.L. Moore, Composite properties for E-glass fibres in a room temperature curable epoxy matrix, Composites 9 (2) (1978) 93–99.
[48] F. Di Caprio, D. Cristillo, S. Saputo, M. Guida, A. Riccio, Crashworthiness of wing leading edges under bird impact event, Compos. Struct. 216 (2019) 39–52.
[49] Y. Chen, S. Hou, K. Fu, X. Han, L. Ye, Low-velocity impact response of composite sandwich structures: modelling and experiment, Compos. Struct. 168 (2017) 322–334.
[50] E.J. Barbero, M. Shahbazi, Determination of material properties for ANSYS progressive damage analysis of laminated composites, Compos. Struct. 176 (2017) 768–779.
[51] G.-C. Yu, L.-Z. Wu, L. Ma, J. Xiong, Low velocity impact of carbon fiber aluminum laminates, Compos. Struct. 119 (2015) 757–766.
[52] Ansys_help. www.ansyshelp.ansys.com, 2019.
[53] A.U. Ude, A.K. Ariffin, C.H. Azhari, Impact damage characteristics in reinforced woven natural silk/epoxy composite face-sheet and sandwich foam, coremat and honeycomb materials, Int. J. Impact Eng. 58 (2013) 31–38.
[54] L. Gemi, N. Tarakçioğlu, A. Akdemir, Ö.S. Şahin, Progressive fatigue failure behavior of glass/epoxy (±75)2 filament-wound pipes under pure internal pressure, Mater. Des. 30 (10) (2009) 4293–4298.
[55] A.J. Malcom, M.T. Aronson, V.S. Deshpande, H.N.G. Wadley, Compressive response of glass fiber composite sandwich structures, Compos. Appl. Sci. Manuf. 54 (2013) 88–97.

[56] M.S. Han, J.U. Cho, Impact damage behavior of sandwich composite with aluminum foam core, Trans. Nonferrous Metals Soc. China 24 (2014) s42–s46.
[57] T. Anderson, E. Madenci, Experimental investigation of low-velocity impact characteristics of sandwich composites, Compos. Struct. 50 (3) (2000) 239–247.
[58] K.B. Shin, J.Y. Lee, S.H. Cho, An experimental study of low-velocity impact responses of sandwich panels for Korean low floor bus, Compos. Struct. 84 (3) (2008) 228–240.